



**HAL**  
open science

## One-Dimensional Anderson Localization in Certain Correlated Random Potentials

Pierre Lugan, Alain Aspect, Laurent Sanchez-Palencia, Dominique Delande, Benoît Grémaud, Cord A. Müller, Christian Miniatura

► **To cite this version:**

Pierre Lugan, Alain Aspect, Laurent Sanchez-Palencia, Dominique Delande, Benoît Grémaud, et al.. One-Dimensional Anderson Localization in Certain Correlated Random Potentials. 2009. hal-00357700v2

**HAL Id: hal-00357700**

**<https://hal.science/hal-00357700v2>**

Preprint submitted on 3 Feb 2009 (v2), last revised 13 Aug 2009 (v3)

**HAL** is a multi-disciplinary open access archive for the deposit and dissemination of scientific research documents, whether they are published or not. The documents may come from teaching and research institutions in France or abroad, or from public or private research centers.

L'archive ouverte pluridisciplinaire **HAL**, est destinée au dépôt et à la diffusion de documents scientifiques de niveau recherche, publiés ou non, émanant des établissements d'enseignement et de recherche français ou étrangers, des laboratoires publics ou privés.

# One-Dimensional Anderson Localization in Certain Correlated Random Potentials

P. Lukan, A. Aspect, and L. Sanchez-Palencia

Laboratoire Charles Fabry de l'Institut d'Optique, CNRS and Univ. Paris-Sud,  
Campus Polytechnique, RD 128, F-91127 Palaiseau cedex, France

D. Delande<sup>1</sup>, B. Grémaud<sup>1,2,3</sup>, C.A. Müller<sup>1,4</sup>, and C. Miniatura<sup>2,3,5</sup>

<sup>1</sup>Laboratoire Kastler-Brossel, UPMC, ENS, CNRS; 4 Place Jussieu, F-75005 Paris, France

<sup>2</sup>IPAL, CNRS; 1 Fusionopolis Way, Singapore 138632, Singapore

<sup>3</sup>Centre for Quantum Technologies, National University of Singapore, 3 Science Drive 2, Singapore 117543, Singapore

<sup>4</sup>Physikalisches Institut, Universität Bayreuth, D-95440 Bayreuth, Germany

<sup>5</sup>Institut Non Linéaire de Nice, UNS, CNRS; 1361 route des Lucioles, F-06560 Valbonne

(Dated: February 3, 2009)

We investigate Anderson localization of ultracold atoms in weak 1D correlated random potentials resulting from laser speckles. We show the existence of effective mobility edges corresponding to sharp crossovers between regions where localization lengths differ by orders of magnitude. Using perturbation theory, we derive analytical formulas up to two orders beyond Born approximation and find them in excellent agreement with exact numerical calculations. Finally, we analyze our findings in the light of a diagrammatic approach.

PACS numbers: 03.75.-b,42.25.Dd,72.15.Rn

Anderson localization (AL) of single electron wave functions [1], first proposed to understand certain metal-insulator transitions, is now considered a ubiquitous phenomenon, which can happen for any kind of waves propagating in a medium with random impurities [2, 3]. It can be understood as a coherent interference effect in multiple scattered waves from random defects, yielding localized waves with an exponential profile, and resulting into complete suppression of the usual diffusive transport associated with incoherent wave scattering [4].

So far, AL has been reported for light waves in diffusive media [5, 6] or photonic crystals [7, 8], sound waves [9], microwaves [10]. Ultracold atoms have allowed study of AL in momentum space [11, 12], and recently it has been possible to directly observe localized atomic matter waves [13, 14]. In the latter case, random potentials can be controlled [15, 16, 17], offering unprecedented possibilities to explore the role of finite-range correlations.

Systems in 1D are peculiar as regards AL compared to higher dimensions. In 3D, there is a metal-insulator transition (*mobility edge*) given approximately by the Ioffe-Regel criterion,  $kl^* \sim 1$  [18], i.e. only states with a wavenumber  $k$  smaller than the inverse transport mean-free path  $l^*$  are localized. In 2D, all states are localized but the localization length  $L_{\text{loc}}$  diverges exponentially with  $kl^*$  for  $kl^* > 1$ . In contrast, there is no localization threshold in 1D and  $L_{\text{loc}}$  is proportional to  $l^*$  [19]. However, long-range correlations can induce anomalous diffusion and non-standard localization properties [20].

Important examples are random potentials resulting from laser speckles [21] and used in experiments with ultracold atoms [13]. Their power spectrum have a finite support so that there is no Fourier component beyond a certain value  $2k_c$ . Then, the Born approximation—which is expected to be relevant for weak disorder [22]—pre-

dicts that the random potential does not provide back-scattering and thus no localization for  $k > k_c$ . This property defines an *effective mobility edge* in 1D [23] at  $k = k_c$ , evidences of which have been reported [13, 24]. In this context, questions have raised about the true nature of the *effective mobility edge* and localization properties beyond it. Related questions have been addressed in different contexts [25] but speckle potentials have non-standard properties: (i) They are non-Gaussian disorders [26] and (ii) their probability distribution is not symmetric. These make them an original class of disorder with odd terms in the Born expansion (see below).

In this Letter, we address these questions for speckle potentials using perturbation theory beyond the Born approximation and exact numerical calculations [27]. We

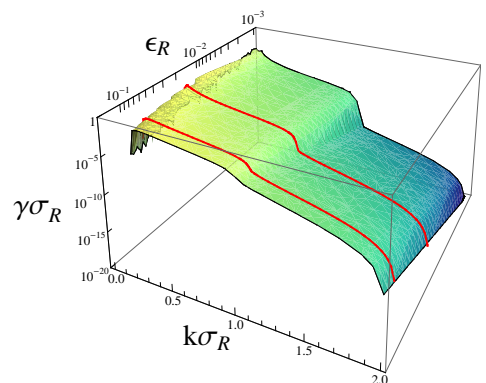


Figure 1: (color online) Lyapunov exponent  $\gamma$  calculated two orders beyond Born approximation versus the particle momentum  $k$  and the strength of disorder  $\epsilon_R$  for particles in 1D speckle potentials created with a square diffusive plate. The red lines correspond to  $\epsilon_R = 0.1$  and  $\epsilon_R = 0.02$  respectively (same curves as in Fig. 3).

find that AL occurs even beyond the effective mobility edge at  $k = k_c$ . In fact, there exist several effective mobility edges located at  $k_c^{(p)} = pk_c$  with  $p$  an integer such that AL in the successive regions  $k_c^{(p-1)} < k < k_c^{(p)}$  is dominated by higher and higher order scattering processes. *Effective mobility edges* are thus characterized by sharp crossovers in the  $k$ -dependence of the Lyapunov exponent (see Fig. 1). We prove it for the first two effective mobility edges by calculating explicitly the three lowest orders in the Born expansion. Our analytic calculations are in excellent agreement with numerics. Finally, we analyze our findings using diagrammatic methods.

*Phase formalism* – Consider a particle of energy  $E$  in a 1D random potential  $V(z)$  of statistical average zero ( $\langle V \rangle = 0$ ). We use the phase formalism [22]:

$$\phi(z) = r(z) \sin[\theta(z)]; \quad \partial_z \phi = kr(z) \cos[\theta(z)], \quad (1)$$

with  $k = \sqrt{2mE/\hbar^2}$  the particle wavenumber in the absence of disorder, for which the Schrödinger equation in 1D is equivalent to the coupled equations

$$\partial_z \theta(z) = k [1 - (V(z)/E) \sin^2(\theta(z))] \quad (2)$$

$$\ln[r(z)/r(0)] = k \int_0^z dz' (V(z')/2E) \sin(2\theta(z')). \quad (3)$$

The phase formalism allows us to solve Eq. (2) perturbatively in powers of  $V$ , and to reintroduce the solutions at different orders into Eq. (3). This yields the corresponding perturbation orders of the Lyapunov exponent:

$$\gamma(k) = \lim_{|z| \rightarrow \infty} \langle \ln(r(z))/|z| \rangle = \sum_{n \geq 2} \gamma^{(n)}(k). \quad (4)$$

The  $n$ -th order term,  $\gamma^{(n)}$ , is thus expressed as a function of the  $n$ -point correlator  $C_n(z_1, \dots, z_{n-1}) = \langle V(0)V(z_1)\dots V(z_{n-1}) \rangle$  of the random potential. Up to second order beyond the Born term ( $n = 4$ ), we find

$$\gamma^{(n)} = \sigma_R^{-1} \left( \frac{\epsilon_R}{k\sigma_R} \right)^n f_n(k\sigma_R) \quad (5)$$

where  $\epsilon_R = 2m\sigma_R^2 V_R/\hbar^2$  and

$$f_2(\kappa) = +\frac{1}{4} \int_{-\infty}^0 du c_2(u) \cos(2\kappa u) \quad (6)$$

$$f_3(\kappa) = -\frac{1}{4} \int_{-\infty}^0 du \int_{-\infty}^u dv c_3(u,v) \sin(2\kappa v) \quad (7)$$

$$f_4(\kappa) = -\frac{1}{8} \int_{-\infty}^0 du \int_{-\infty}^u dv \int_{-\infty}^v dw c_4(u,v,w) \times \{2 \cos(2\kappa w) + \cos[2\kappa(v+w-u)]\}. \quad (8)$$

Reduced correlators,  $c_n$ , are defined using amplitude  $V_R$  and correlation length  $\sigma_R$  of the disorder (precisely defined below) as unit scales:  $C_n(z_1, \dots, z_{n-1}) = V_R^n c_n(z_1/\sigma_R, \dots, z_{n-1}/\sigma_R)$ . Notice that the compact form

of Eq. (8) is valid provided that oscillating terms, which may appear from contributions of  $c_4$  that can be factorized as correlators  $c_2$ , are appropriately regularized at infinity. In Eq. (5), the coefficients  $(\epsilon_R/k\sigma_R)^n$  diverge in the low-momentum limit  $k \rightarrow 0$  while it is known that the exact  $\gamma(k)$  remains finite for any finite  $\epsilon_R$  [28]. This indicates a breakdown of the perturbative Born expansion, which is known to be valid when  $\gamma(k) \ll k$ , that is when the localization length is much larger than the particle wavelength, a physically satisfactory criterion.

For zero-range correlations, i.e. for  $c_2(u) \propto \delta(u)$ , the Born term,  $\gamma^{(2)}(k)$ , does not vanish and is thus the leading order for any  $k \gg \gamma^{(2)}(k)$ . In random potentials with long-range correlations, such as speckle potentials, the situation happens to be richer.

*Speckle potentials* – Speckle patterns are obtained by transmission of a laser beam through a medium with a random phase profile, such as a ground glass plate. The resulting complex electric field,  $\mathcal{E}$ , is a sum of independent random variables, and is thus a Gaussian process. In such a light field, atoms experience a random potential proportional to the light intensity,  $|\mathcal{E}|^2$ . Defining the zero of energies so that  $\langle V \rangle = 0$ , the random potential is

$$V(z) = V_R \times (|a(z/\sigma_R)|^2 - \langle |a(z/\sigma_R)|^2 \rangle). \quad (9)$$

Depending on the detuning of the laser with respect to the atomic resonance, the sign of  $V_R$  can be either positive (‘blue detuning’) or negative (‘red detuning’). The quantities  $a(u)$  are complex Gaussian variables, proportional to the electric fields,  $\mathcal{E}$ . Notice that all correlators,  $c_n$ , of the random potential are completely determined by the sole field-field correlator  $c_a(u) = \langle a(0)^* a(u) \rangle$  through the statistical Gaussian theorem,

$$\langle a_1^* \dots a_p^* \times a_{p+1} \dots a_{p+p} \rangle = \sum_{\Pi} \langle a_1^* a_{p+\Pi(1)} \rangle \dots \langle a_p^* a_{p+\Pi(p)} \rangle, \quad (10)$$

where  $a_{p'} = a(z_{p'}/\sigma_R)$  and  $\Pi$  describes all  $p!$  permutations of  $[1\dots p]$ . For instance,  $c_2(u) = |c_a(u)|^2$  and defining  $a(u)$  so that  $\langle |a(u)|^2 \rangle = 1$ , we have  $\sqrt{\langle V(z)^2 \rangle} = |V_R|$ . Since speckles result from interferences between light waves of wavelength  $\lambda_L$  coming from a finite size aperture of angular width  $2\theta$ , the Fourier transform of the field-field correlator has no component beyond  $k_c = 2\pi \sin \theta / \lambda_L$  and  $c_a$  has always a finite support:

$$\hat{c}_a(q) = 0 \quad \text{for } |q| > k_c \sigma_R \equiv 1. \quad (11)$$

*Analytic results* – We now apply perturbation theory within the phase formalism up to two orders beyond Born approximation ( $n = 4$ ) for speckle potentials. The discussion below can be generalized to any kind of 1D random potentials that fulfill the sole conditions (9)-(11) with similar conclusions (only formulas for the functions  $f_n(\kappa)$  would change). However, for clarity, we restrict our discussion to 1D speckle potentials created by square

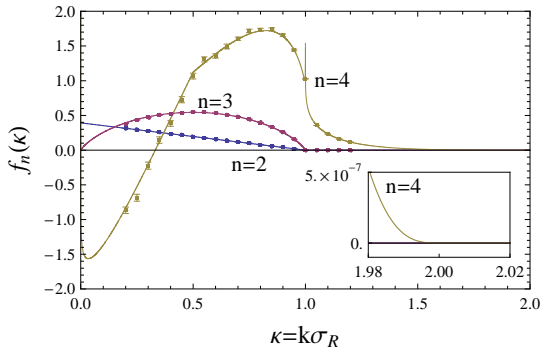


Figure 2: (color online) Functions  $f_n$  for  $n = 2, 3$  and  $4$  for a speckle potential created with a square diffusive plate (i.e.  $c_a(u) = \sin(u)/u$ ). The solid lines correspond to Eqs. (12)-(14) and the points with errorbars to numerical calculations. The inset is a magnification of function  $f_4$  around  $\kappa = 2$ .

diffusive plates as in Ref. [13] for which  $c_a(u) = \sin(u)/u$  and  $\hat{c}_a(q) \propto \Theta(1 - |q|)$  where  $\Theta$  is the Heaviside function. Inserting this correlator into Eqs. (6)-(8), we find

$$f_2(\kappa) = \frac{\pi}{8} \Theta(1 - \kappa)(1 - \kappa) \quad (12)$$

$$f_3(\kappa) = -\frac{\pi}{4} \Theta(1 - \kappa) [(1 - \kappa) \ln(1 - \kappa) + \kappa \ln(\kappa)] \quad (13)$$

$$f_4(\kappa) = \frac{\pi}{64} \left\{ \Theta(1/2 - \kappa) f_4^{0, \frac{1}{2}}(\kappa) + \Theta(1 - \kappa) f_4^{0, 1}(\kappa) + \Theta(\kappa - 1) \Theta(2 - \kappa) f_4^{1, 2}(\kappa) \right\}. \quad (14)$$

The functions  $f_2$  and  $f_3$  are simple and vanish for  $\kappa > 1$  (see Fig. 2). This property is responsible for the existence of the effective mobility edge at  $k = k_c$  [23] such that  $\gamma(k)\sigma_R \sim (\epsilon_R/k\sigma_R)^2$  for  $k \lesssim \sigma_R^{-1}$  while  $\gamma(k)\sigma_R = O(\epsilon_R/k\sigma_R)^4$  for  $k \gtrsim \sigma_R^{-1}$ . Notice that  $f_3(\kappa)$  does not vanish everywhere, a consequence of the non-symmetric probability distribution in speckle potentials. The function  $f_4(\kappa)$  has three components with three different supports:  $f_4^{0, \frac{1}{2}}(\kappa)$  on  $[0, 1/2]$ ,  $f_4^{0, 1}(\kappa)$  on  $[0, 1]$  and  $f_4^{1, 2}(\kappa)$  on  $[1, 2]$ . The formulas for  $f_4^{\alpha, \beta}(\kappa)$  being quite complicated we do not reproduce them [29]. The behavior of  $f_4$  is clearer when plotted (see Fig. 2). The first cut-off is responsible for the discontinuity of the derivative of  $f_4$  at  $\kappa = 1/2$ . At the second cut-off,  $\kappa = 1$ , we find a logarithmic divergence,  $f_4(\kappa) \sim -2 \ln|1 - \kappa|$  which signals a singularity of the perturbative expansion. In addition, it is very narrow (notice that it does not appear in Fig. 1 due to the finite grid of the 3D plot) so we disregard it in the remainder of the Letter. The last cut-off at  $\kappa = 2$  defines the edge of the support of the fourth-order term at  $k = 2\sigma_R^{-1}$ , showing explicitly the existence of a second effective mobility edge at  $k = 2\sigma_R^{-1}$ , such that  $\gamma(k)\sigma_R \sim (\epsilon_R/k\sigma_R)^4$  for  $k \lesssim 2\sigma_R^{-1}$  while  $\gamma(k)\sigma_R = O(\epsilon_R/k\sigma_R)^6$  for  $k \gtrsim 2\sigma_R^{-1}$ . Notice that, although the odd- $n$  terms do not vanish, they cannot be

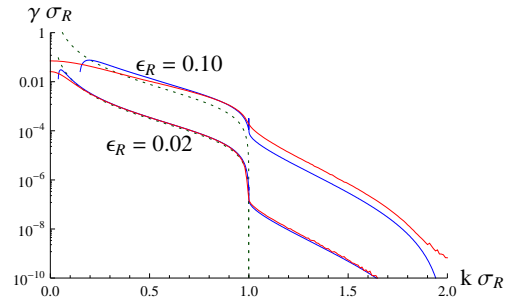


Figure 3: (color online) Lyapunov exponent  $\gamma(k)$  versus the particle momentum  $k$  as determined by exact numerical calculations (red solid line) and comparison to perturbation theory up to two orders beyond Born approximation (i.e. up to  $n = 4$ ; blue solid line). The green dashed lines are the Born term. These results hold for a speckle potential created with a square diffusive plate for two values of the parameter  $\epsilon_R$ .

leading terms in any range of  $k$  owing to the positivity of the Lyapunov exponent irrespective to the sign of  $V_R$ .

*Numerics* – We have also performed exact numerical calculations using a transfer matrix approach. The results are plotted in Fig. 3 for parameters relevant for Ref. [13]:  $\epsilon_R = 0.02$  corresponds to  $V_R/\hbar = 2\pi \times 16\text{Hz}$  in Fig. 3 of Ref. [13] and  $\epsilon_R = 0.1$  to  $V_R/\hbar = 2\pi \times 80\text{Hz}$  in Fig. 3 and to Fig. 4 of Ref. [13]. For  $\epsilon_R = 0.02$ , the agreement between perturbation theory and exact numerical results is excellent. In particular, the effective mobility edge at  $k = \sigma_R^{-1}$  is very clear: We find a sharp step for  $\gamma(k)$  of about two orders of magnitude. The curve corresponding to  $\epsilon_R = 0.1$  shows the same trend but with a smoother and smaller step (about one order of magnitude). Although the Born approximation for  $k \lesssim \sigma_R^{-1}$  and the fourth-order term for  $k \gtrsim \sigma_R^{-1}$  provide reasonable estimates (up to a factor of about 2), higher order terms cannot be neglected. Only near  $k = 0$  is perturbation theory unusable as expected from our discussion above.

In order to check the validity of the analytic formulas (12)-(14), we use a series of calculations of the Lyapunov exponent at fixed  $k$  and various  $\epsilon_R$  that we fit in powers of  $\epsilon_R/k\sigma_R$ . As shown in Fig. 2, the agreement with the analytic expressions is excellent. In particular, the numerics faithfully reproduce the predicted kink at  $\kappa = 1/2$ . The logarithmic singularity around  $\kappa = 1$  is very narrow; we did not attempt to study it in detail.

*Diagrammatic analysis* – Diagrammatic methods provide simple graphical representations of the backscattering processes encoded in Eqs. (6)-(8) and allow to identify *effective mobility edges* quite simply. In 1D,  $L_{\text{loc}} = l^*$  can be calculated from the backscattering probability of  $\langle |\psi|^2 \rangle$  using standard quantum transport theory. The irreducible diagrams of elementary scattering processes in speckle potentials have been identified in Ref. [16].

To lowest order in  $\epsilon_R$  (Born approximation), the aver-

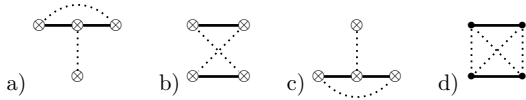


Figure 4: Relevant fourth-order backscattering contributions. Contrary to the case of uncorrelated potentials [30, 31], the sum of diagrams (a)-(c) *does not* give zero for speckle potentials; only diagrams (b) and (d) contribute for  $k\sigma_R \in [1, 2]$ .

age intensity of a plane wave with wave vector  $k$  backscattered by the random potential is described by

$$U_2(k) = \begin{array}{c} k \rightarrow \leftarrow k \\ \swarrow \quad \searrow \\ q+k \quad q-k \\ \nwarrow \quad \nearrow \\ k \leftarrow \rightarrow k \end{array} =: \begin{array}{c} k \rightarrow \leftarrow k \\ \downarrow 2k \\ k \leftarrow \rightarrow k \end{array} . \quad (15)$$

The upper part of the diagram represents  $\psi$  (particle) and the lower part its conjugate  $\psi^*$  (hole). The dotted line  $\bullet \cdots \overset{q}{\curvearrowright} \cdots \bullet = \epsilon_R \hat{c}_a(q)$  represents the field correlator; simple closed loops over field correlations can be written as a potential correlation  $\otimes \cdots \otimes$ . Backscattering requires the diagram (15) to channel a momentum  $2k$ , entering at the particle, down along the potential correlations to the hole. Therefore, the diagram vanishes for  $k\sigma_R > 1$ .

At order  $\epsilon_R^3$ , the only possible contribution is

$$U_3(k) = \begin{array}{c} k \rightarrow \leftarrow k \\ \swarrow \quad \searrow \\ q+k \quad q-k \\ \nwarrow \quad \nearrow \\ k \leftarrow \rightarrow k \end{array} + c.c. \quad (16)$$

The straight black line stands for the particle propagator  $[E_k - E_p + i0]^{-1}$  at intermediate momentum  $p$ . The diagram (16) features two vertical field correlation lines, just as diagram (15), and thus vanishes at the same threshold  $k = \sigma_R^{-1}$ . Evaluating the two-loop diagram (16), we recover precisely the contribution (13).

Many diagrams contribute to order  $\epsilon_R^4$ . First there are the usual backscattering contributions with pure intensity correlations, shown in Fig. 4(a)-(c). Both 4(a) and (c) have a single vertical intensity correlation and vanish for  $k > \sigma_R^{-1}$ . In contrast, the crossed diagram 4(b) has two vertical intensity correlation lines and can thus accommodate momenta up to  $k = 2\sigma_R^{-1}$ . Performing the integration, we find that this diagram reproduces the complicated functional dependence of those contributions to  $f_4^{1,2}$  in Eq. (14) that contain factorized correlators.

Second, there are nine more diagrams, all with non-factorizable field correlations [16]. A single one has not two, but four vertical field correlation lines, shown in Fig. 4(d), and contributes for  $k\sigma_R \in [1, 2]$ . Carrying out the three-loop integration, we recover exactly the non-factorizable contributions to  $f_4^{1,2}$  in Eq. (14).

*Conclusion* – We have shown that in a speckle potential of correlation length  $\sigma_R$ , the  $k$ -dependence of the Lyapunov exponent exhibits sharp crossovers (*effective*

*mobility edges*) separating regions where AL is due to higher and higher order scattering processes. We have shown explicitly the existence of the first two *effective mobility edges* at  $k = \sigma_R^{-1}$  and  $k = 2\sigma_R^{-1}$ . We infer that there exists a series of *effective mobility edges* at  $k_c^{(p)} = p\sigma_R^{-1}$  with  $p$  an integer since generically, diagrams with  $2p$  vertical field correlations or  $p$  intensity correlations can contribute up to  $k = p\sigma_R^{-1}$ .

Stimulating discussions with P. Bouyer, V. Josse, T. Giamarchi and B. van Tiggelen are acknowledged. This research was supported by the French CNRS, ANR, MENRT, Triangle de la Physique and IFRAF.

- 
- [1] P.W. Anderson, Phys. Rev. **109**, 1492 (1958).
  - [2] E. Akkermans and G. Montambaux, *Mesoscopic Physics of Electrons and Photons* (Cambridge Univ. Press, 2006).
  - [3] B. van Tiggelen, in *Wave Diffusion in Complex Media*, lecture notes at Les Houches 1998, edited by J.P. Fouque, NATO Science (Kluwer, Dordrecht, 1999).
  - [4] P.A. Lee and T.V. Ramakrishnan, Rev. Mod. Phys. **57**, 287 (1985).
  - [5] D.S. Wiersma *et al.*, Nature **390**, 671 (1997).
  - [6] M. Störzer *et al.*, Phys. Rev. Lett. **96**, 063904 (2006).
  - [7] T. Schwartz *et al.*, Nature **446**, 52 (2007).
  - [8] Y. Lahini *et al.*, Phys. Rev. Lett. **100**, 013906 (2008).
  - [9] H. Hu *et al.*, Nature Phys. **4**, 945 (2008).
  - [10] A.A. Chabanov *et al.*, Nature **404**, 850 (2000).
  - [11] J.L. Moore *et al.*, Phys. Rev. Lett. **75**, 4598 (1995).
  - [12] J. Chabé *et al.*, Phys. Rev. Lett. **101**, 255702 (2008).
  - [13] J. Billy *et al.*, Nature **453**, 891 (2008).
  - [14] G. Roati *et al.*, Nature **453**, 895 (2008).
  - [15] D. Clément *et al.*, New J. Phys. **8**, 165 (2006).
  - [16] R.C. Kuhn *et al.*, New J. Phys. **9**, 161 (2007).
  - [17] L. Fallani *et al.*, Adv. At. Mol. Opt. Phys. **56**, 119 (2008).
  - [18] A.F. Ioffe and A.R. Regel, Prog. Semicond. **4**, 237 (1960).
  - [19] C.W.J. Beenakker, Rev. Mod. Phys. **69**, 731 (1997).
  - [20] F.M. Izrailev and A.A. Krokhin, Phys. Rev. Lett. **82**, 4062 (1999).
  - [21] J.W. Goodman, *Speckle Phenomena in Optics: Theory and Applications* (Roberts & Co. Pub., 2007).
  - [22] I.M. Lifshits *et al.*, *Introduction to the Theory of Disordered Systems* (Wiley and sons, New York, 1988).
  - [23] L. Sanchez-Palencia *et al.*, Phys. Rev. Lett. **98**, 210401 (2007); New J. Phys. **10**, 045019 (2008).
  - [24] This effect occurs only in 1D since in 2D or 3D, any wave can be scattered by a Fourier component of the disorder with arbitrary small momentum, although possibly with a small deflection angle [16].
  - [25] L. Tessieri, J. Phys. A: Math. Gen. **35**, 9585 (2002).
  - [26] In laser speckles, the random potential, which is proportional to the square of the modulus of a complex Gaussian process, is not Gaussian [21].
  - [27] While completing this work, we have been informed of a recent similar study; E. Gurevich, arXiv:0901.3125.
  - [28] B. Derrida and E. Gardner, J. Physique **45**, 1283 (1984).
  - [29] Our formulas are provided as EPAPS Auxiliary Material.
  - [30] I.V. Gornyi *et al.*, Phys. Rev. B **75**, 085421 (2007).
  - [31] A. Cassam-Chenai, and B. Shapiro, J. Phys. I France **4**, 1527 (1994).



**AUXILIARY MATERIAL**

The functions  $f_4^{\alpha,\beta}$  read

$$\begin{aligned}
f_4^{0,\frac{1}{2}}(\kappa) &= -4\pi^2(1-2\kappa) \\
f_4^{0,1}(\kappa) &= 4 - 6\kappa - \frac{10\pi^2}{3}(1-2\kappa) - (4-2\kappa)\ln(\kappa) \\
&\quad - \left(\frac{5}{\kappa} - 3\kappa\right)\ln(1-\kappa) + \left(\frac{1}{\kappa} + \kappa\right)\ln(1+\kappa) \\
&\quad - (4-8\kappa)\ln^2(\kappa) + 22(1-\kappa)\ln^2(1-\kappa) \\
&\quad + (18+14\kappa)\ln^2(1+\kappa) \\
&\quad - 16(1-\kappa)\ln(1-\kappa)\ln(\kappa) \\
&\quad - 4(1-\kappa)\ln(1-\kappa)\ln(1+\kappa) \\
&\quad - 32(1+\kappa)\ln(\kappa)\ln(1+\kappa) \\
&\quad - 24(1+\kappa)\text{Li}_2(\kappa) + 32(1+\kappa)\text{Li}_2\left(\frac{\kappa}{1+\kappa}\right) \\
&\quad - 8\kappa\text{Li}_2\left(\frac{2\kappa}{1+\kappa}\right) - 8(1-2\kappa)\text{Li}_2\left(2-\frac{1}{\kappa}\right) \\
f_4^{1,2}(\kappa) &= -4 + 2\left(1 + \frac{\pi^2}{3}\right)\kappa + 8\kappa\text{Li}_2(1-\kappa) \\
&\quad - \left(\frac{4}{\kappa} - 4 + 2\kappa\right)\ln(\kappa-1) \\
&\quad - 4(\kappa-1)\ln^2(\kappa-1) + 8\kappa\ln(\kappa-1)\ln(\kappa)
\end{aligned}$$

where  $\text{Li}_2 = \int_z^0 dt \ln(1-t)/t = \sum_{k=1}^{\infty} z^k/k^2$  is the dilogarithm function.